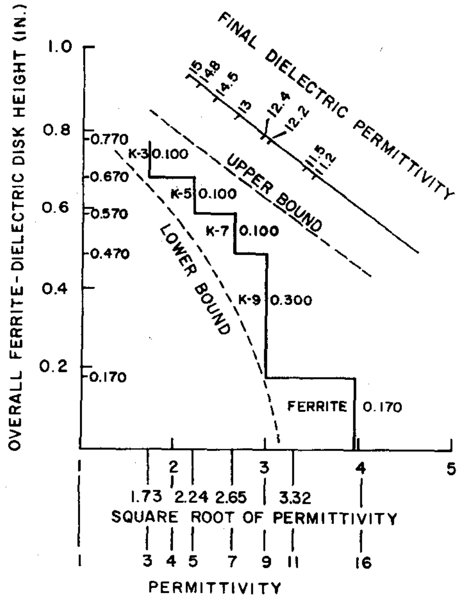

Fig. 4. Dielectric loading nomogram.

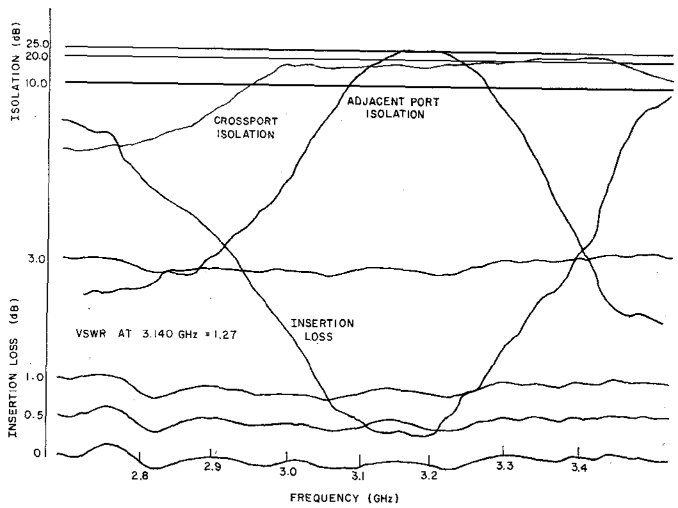

Fig. 5. Low-level insertion loss and isolation.

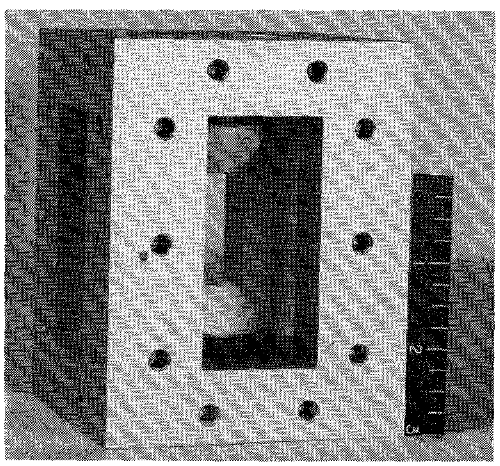

Fig. 6. E-plane four-port junction circulator.

figuration, and the insertion loss does not exceed 0.5 dB at either low- or high-power operation at 3140 MHz. In addition, a 1.0-dB bandwidth of 210 MHz (6.7 percent) and a 3.0-dB bandwidth of 470 MHz (15 percent) have been realized. High-power operation at the rated power levels has been achieved in a room-temperature environment without the need for external cooling. The required magnetic biasing field is only 400 G, indicating that a practical device, incorporating a compact permanent magnet circuit, is feasible. The final device easily provides the desired high-power, compact, lightweight package.

Edward E. DeCamp, Jr.
Robert M. True
Electron Tubes Division
Electronic Components Labs.
U. S. Army Electronics Command
Fort Monmouth, N. J. 07703

References

[1] B. A. Auld, "The synthesis of symmetrical waveguide circulators," *IRE Trans. Microwave Theory Tech.*, vol. MTT-7, Apr. 1959, pp. 238–246.
[2] C. E. Fay and R. L. Comstock, "Operation of the ferrite junction circulator," *IEEE Trans. Microwave Theory Tech.*, vol. MTT-13, Jan. 1965, pp. 15–27.
[3] L. E. Davis and S. R. Longley, "E-plane 3-port X-band waveguide circulators," *IEEE Trans. Microwave Theory Tech.* (Corresp.), vol. MTT-11, Sept. 1963, pp. 443–445.
[4] W. H. Wright, Jr., and J. W. McGowan, "High-power Y-junction E-plane circulator," *IEEE Trans. Microwave Theory Tech.* (Corresp.), vol. MTT-16, Aug. 1968, pp. 557–559.
[5] S. R. Longley, "Experimental 4-port E-plane junction circulators," *IEEE Trans. Microwave Theory Tech.* (Corresp.), vol. MTT-15, June 1967, pp. 378–380.

A 360° Reflection-Type Diode Phase Modulator

***Abstract*—A 360° phase modulator using two series-tuned varactors in a parallel connection is described. The design minimizes the change in total phase shift with frequency and gives a small attenuation ripple. The modulator is centered at 2 GHz and gives a total phase shift at 360° at the center frequency, an attenuation ripple of 1.3 dB over a 10-percent bandwidth and a 7° decrease of phase shift at the band edges.**

Phase modulators of the reflection type using hybrids or circulators are well known. Garver [1], [2] has given designs of phase modulators with a phase shift of 360°. A simple reflection-type phase modulator which uses two varactor diodes to obtain a full 360° phase shift will be described.

The diode is represented by a capacitance, voltage tunable between $C_{\max}$ and $C_{\min}$ and a loss resistance r. Each of the diodes is series tuned with an inductance, so that one diode circuit is series resonant at a low bias voltage associated with $C_{\max}$, and the other diode circuit is series resonant at a high bias voltage associated with $C_{\min}$. The two diode circuits are connected in parallel. The low bias resonance circuit gives a voltage-dependent reactance X_1, and the high bias resonance gives a voltage-dependent reactance X_2. The reactance range between bias extremes is

$$\Delta X = \frac{1}{\omega_0 C_{\min}} - \frac{1}{\omega_0 C_{\max}}$$

where ω_0 is the center frequency. At the bias point, where the two reactances are equal but opposite, parallel resonance occurs with an equivalent parallel resistance:

$$R_p = \frac{1}{8}\,\frac{(\Delta X)^2}{r}. \tag{1}$$

Manuscript received June 4, 1970; revised Septemper 21, 1970.

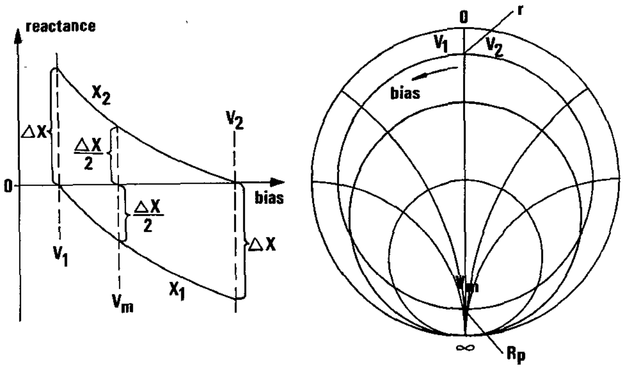

Fig. 1. Voltage dependence for diode circuit and complete parallel circuit.

The voltage dependence of the two reactances are shown in Fig. 1 together with a Smith-chart plot of the voltage dependence of the complete parallel circuit.

The parallel circuit is connected to a $\lambda/4$ transformer with a characteristic impedance of $Z_{\lambda/4}$ so chosen that r and R_p will give the same reflection coefficient in a 50-Ω line:

$$Z_{\lambda/4}^2 = 50\sqrt{rR_p}. \tag{2}$$

This gives a power reflection coefficient $|\rho|^2$ at the series and parallel resonances of

$$|\rho|^2 \approx 1 - 11.3\frac{r}{\Delta X}. \tag{3}$$

The Smith-chart plot of the complete circuit does not follow a constant ρ circle but rather a constant r circle at low and high bias voltages. Thus a certain fluctuation in the reflection coefficient is unavoidable. The minimum power reflection coefficient is given by

$$|\rho_{\min}|^2 \approx 1 - 13.3\frac{r}{\Delta X}. \tag{4}$$

It is of interest to investigate how the total phase shift between the bias points is affected by frequency. The change in total phase shift can be determined from the change in phase at the bias extremes. At the bias extremes one of the two diode circuits is series resonant with a small reactance. A small reactance gives a linear relation between change in phase and change in reactance with frequency. For the low and high bias series resonances the incremental reactances are given by

$$\delta X_1 = 2\frac{1}{\omega_0 C_{\max}}\frac{\delta\omega}{\omega_0}$$

$$\delta X_2 = 2\frac{1}{\omega_0 C_{\min}}\frac{\delta\omega}{\omega_0}. \tag{5}$$

The change in total phase shift is given by

$$\delta\phi = 2\frac{\delta X_1 - \delta X_2}{\sqrt{rR_p}} \tag{6}$$

which combined with (1) and (5) gives

$$\delta\phi = -8\sqrt{2}\frac{\delta\omega}{\omega_0}. \tag{7}$$

From (7) it follows that the total phase shift varies linearly with frequency, which is not desirable for wide band-width. From (6) it follows that if the reactance slope of the two series resonances is the same, the change in total phase shift can be minimized. This can be accomplished by connecting a series-resonant circuit containing a capacitance C_0 in series with the low bias resonance circuit. The capacitance C_0 is chosen to equalize the reactance slopes:

$$\frac{1}{C_0} = \frac{1}{C_{\min}} - \frac{1}{C_{\max}}. \tag{8}$$

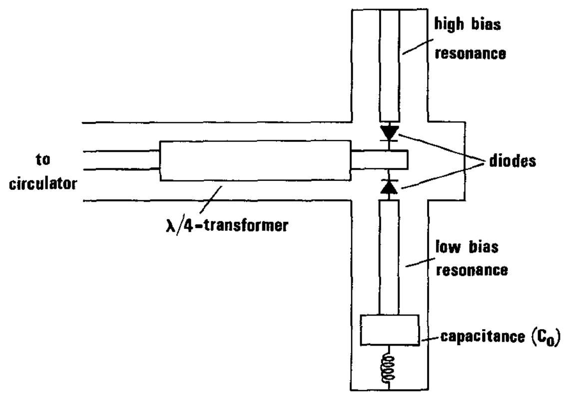

Fig. 2. Practical realization of phase modulator.

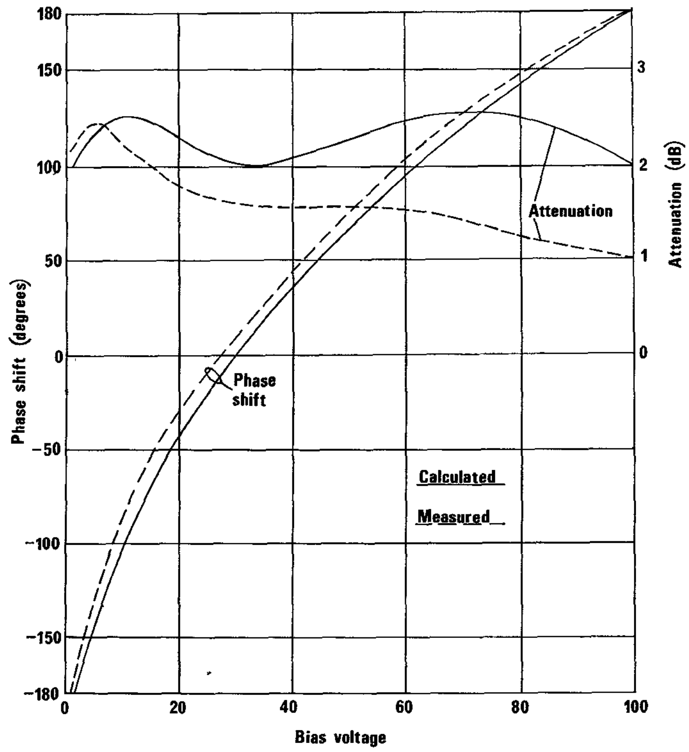

Fig. 3. Calculated and measured phase shift and attenuation at 2 GHz as functions of bias.

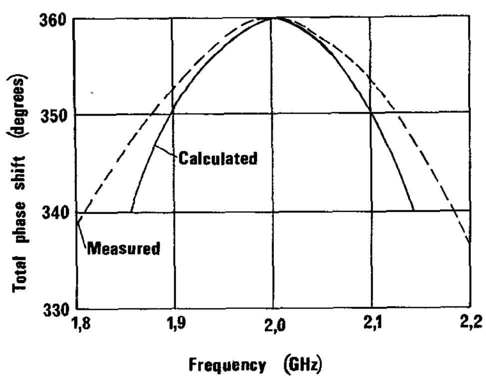

Fig. 4. Calculated and measured total phase shift as functions of frequency.

For the low and high bias resonance this gives

$$\delta X_1 = 2\frac{1}{\omega_0 C_{\min}}\frac{\delta\omega}{\omega_0} - 4\frac{1}{\omega_0 C_{\min}}\left(\frac{C_{\max}}{C_{\max}-C_{\min}}\right)\left(\frac{\delta\omega}{\omega_0}\right)$$

$$\delta X_2 = 2\frac{1}{\omega_0 C_{\min}}\frac{\delta\omega}{\omega_0} + 4\frac{1}{\omega_0 C_{\min}}\left(\frac{C_{\max}}{C_{\max}-C_{\min}}\right)\left(\frac{\delta\omega}{\omega_0}\right)^2 \quad (9)$$

which when inserted in (6) gives

$$\delta\phi = -32\sqrt{2}\left(\frac{C_{\max}}{C_{\max}-C_{\min}}\right)^2\left(\frac{\delta\omega}{\omega_0}\right)^2. \quad (10)$$

The practical phase modulator is realized in a coaxial structure as shown in Fig. 2.

The phase shifter is designed for 2 GHz and uses varactors with a breakdown voltage of 100 V and a cutoff frequency of 80 GHz at breakdown. The phase shifter is voltage tunable between 1.3 and 100 V, which gives $C_{\max}=6.4$ pF and $C_{\min}=1.4$ pF. The calculated and measured phase shift and attenuation at 2 GHz as functions of bias are shown in Fig. 3. The calculated and measured total phase shift as functions of frequency are shown in Fig. 4.

Bengt T. Henoch
Peter Tamm
Microwave Dep.
Royal Institute of Technology
Stockholm, Sweden

References

[1] R. V. Garver, "Broadband binary 180° diode phase modulators," *IEEE Trans. Microwave Theory Tech.*, vol. MTT-13, Jan. 1965, pp. 32–38.
[2] ——, "360° varactor linear phase modulator," *IEEE Trans. Microwave Theory Tech.*, vol. MTT-17, Mar. 1969, pp. 137–147.

A Comparison of Two Nonreciprocal Latching Phaser Configurations

***Abstract*—The microwave and switching characteristics of the rectangular-toroid latching-ferrite-phaser configuration are compared and contrasted with those of the circumferentially magnetized circular rod in rectangular waveguide.**

We have made an experimental comparison of the performance characteristics of two nonreciprocal latching-ferrite-phaser configurations, namely, the circumferentially magnetized circular rod and the dielectrically loaded rectangular toroid in rectangular waveguide, illustrated in Fig. 1. Both versions have been studied extensively for beam-steering applications in phased-array radar systems [1], [2]. The data presented in this correspondence contrast their relative merits and provide a more convenient basis for selecting the phaser configuration for a specific application than has previously been available.

The pertinent dimensions of the two configurations are given in Fig. 1. The center slot in the rectangular toroid was loaded with magnesium titanate dielectric ($\epsilon' \approx 16$) and the geometry was chosen to yield a peak-power rating in the kilowatt range. The twin-slab model [1] was used as a design guide for estimating electrical performance. The low-cost fabrication and assembly techniques that were utilized have been described elsewhere [3]. The ferrite rod dimensions of the second configuration, which were chosen for practical convenience, yielded a reasonable compromise between RF performance and switching characteristics. Two flat surfaces machined on the sides of the rod provided a good mechanical and thermal connection to the waveguide walls.

Manuscript received June 8, 1970; revised August 5, 1970. This work was sponsored by the Department of the Army.

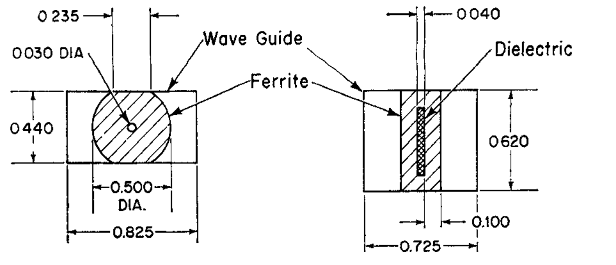

Fig. 1. Geometry of phaser configurations investigated. (a) Rod configuration. (b) Dielectrically loaded rectangular-toroid configuration. All dimensions in inches.

TABLE I

Parameter	Circular Rod Configuration	Dielectrically Loaded Rectangular-Toroid Configuration
Toroid material	TT-1-109	TT-1-109
Dielectric loading	—	Trans-Tech D-16
B_R	880 G	880 G
Center frequency	5.7 GHz	5.7 GHz
Differential phase shift per inch (Δ_φ)	81°	95°
Length of toroid	4.15 in	6 in
Figure of merit	1110°/dB	900°/dB
Peak power threshold	3.5 kW	4.6 kW
Reduction in $\Delta\varphi$ at 250-W incident average power	8 percent	18 percent
Change in insertion phase ($P_{ave}=250$ W)	state 1: −21° state 2: +56°	state 1: −8° state 2: +95°
Drive current to achieve 99 percent B_R	12 A	16 A
Drive current corresponding to $H=H_c$	1.75 A	2.2 A
Switching energy for 360° phaser	180 μJ	115 μJ
Relative ferrite cross-sectional area	1.39	1
f/f_c of LSE_{11} mode	0.83	0.7
f/f_c of LSM_{11} mode	0.96	1.1

The experimental results are summarized in Table I. The small-signal RF performances of the two devices are very similar. The rectangular-toroid version yielded somewhat higher differential phase shift per inch, due to the dielectric loading effect [4], but the figure of merit (degrees phase shift per decibel loss) was slightly lower.

The peak-power threshold P_T was measured using a 60-cycle repetition rate and a 6-μs pulsewidth. The threshold power for the rod configuration was some 24 percent lower than for the rectangular-toroid configuration. This reduction is accountable if one makes allowance for 1) the variation in RF magnetic field intensity with waveguide height and 2) the variation in P_T with dielectric constant ϵ'_d of the loading material [4].

Both phaser configurations were tested at average power levels of up to 250 W. The circular-rod version exhibited greater thermal stability, as measured by the change in insertion phase and differential phase shift. This appears to be attributable to 1) the larger toroidal cross section over which the dissipation is distributed and 2) the smaller waveguide height which provides a shorter source-to-sink path for the heat flow.

In order to compare the switching energy, adequate drive current was applied to each toroid in order to establish a remanent flux equal to 99 percent of B_R for the major hysteresis loop. The rectangular toroid required greater drive—16 A (peak) compared to 12 A (peak). The drive currents corresponding to $H=H_c$ were 2.2 A and 1.75 A, respectively. The ratio of peak switching current is roughly equal to the ratio of the toroid circumferences. The switching energy of 180 μJ per 360° of differential phase shift for the circular-rod version is roughly 50 percent greater than that required for the rectangular-toroid arrangement.